European Congress on Computational Methods in Applied Sciences and Engineering
ECCOMAS 2004
P. Neittaanmäki, T. Rossi, S. Korotov, E. Oñate, J. Périaux, and D. Knörzer (eds.)
Jyväskylä, 24–28 July 2004

OPTIMAL CONTROL METHODS FOR ULTRASOUND SURGERY

Matti Malinen*, Tomi Huttunen*, and Jari P. Kaipio*

*Department of Applied Physics
University of Kuopio, P.O. Box 1627, FIN-70211 Finland
e-mail: Matti.Malinen@uku.fi, web page: http://venda.uku.fi/∼mamaline

Key words: Ultrasound surgery, feedforward control, feedback control, thermal dose, temperature

Abstract. *In this paper, a two-stage control method is proposed to control thermal dose and temperature in ultrasound surgery. The first part in the proposed scheme consists of nonlinear model-based feedforward control. The focusing as well as the scanning path of the foci is chosen by the feedforward controller. The presented feedforward scheme leads to a large dimensional nonlinear control problem which is solved with gradient based algorithm. The temperature measurements during the ultrasound surgery can be adopted from the magnetic resonance imaging (MRI). In the second part of the control scheme these temperature measurements with LQG feedback control and Kalman filter are used to compensate the modeling errors which may arise in the feedforward part. The LQG controller and Kalman filter are derived by linearizing the original nonlinear state equation with respect to the feedforward control trajectories. The presented control scheme is tested with numerical simulations and feasible solutions can be achieved with both feedback and feedforward controllers. In addition, simulations indicate that the LQG scheme can compensate large modeling errors.*

1 INTRODUCTION

As ultrasound propagates in biological tissue, a part of the wave energy is absorbed and changed into heat. The absorbed energy of the ultrasound can be used as a distributed heat source in ultrasound surgery. The main idea of the ultrasound surgery is to raise the temperature or thermal dose in the cancerous tissue to the level that causes necrosis, while temperature in healthy tissue is kept as low as possible to prevent the undesired damage [26, 5, 25]. The main advantages of ultrasound surgery are that it is noninvasive and that there are no side effects as in radiotherapy. However, ultrasound surgery treatment requires accurate control of the temperature and thermal dose distribution so that the desired thermal response in tissues can be achieved.

Several control approaches have been proposed to control the thermal dose in ultrasound surgery. These approaches include temporal switching between the individual focus points [7], optimization of the steady-state power deposition [12] and model predictive control with linearized thermal dose [1]. In addition, MRI-based optimization techniques have been proposed in [8, 21, 23]. These methods use MRI temperature measurements for on-line feedback during the treatment. The main limitations of these earlier control approaches are that they are based on predetermined focus points and scanning path for the foci. In this case control problem reduces to linear form, but there are several limitations in such approach. First, hot spots may arise in healthy tissue due the side lobes of the focused fields, especially if bones coincide with ultrasound field. In addition, diffusion in the proposed schemes is a drawback, since heat is conducted from focus points to healthy tissue during treatment. Furthermore, the accumulated thermal dose when the transducers are turned off is usually neglected. This is an important issue in ultrasound surgery control since thermal dose distribution changes when tissue cools back to ambient temperature.

The purpose of this study is to represent an alternative control procedure to ultrasound surgery treatments. The presented approach consist of two parts. First, model-based feedforward control is used to optimize the thermal dose distribution in tissue. The control variables are the real and imaginary parts of the transducer excitations. These control variables are changed as a function of time to obtain the desired thermal dose distribution in tissues. A quadratic cost criteria is used to weight the thermal dose distribution and the time derivative of the transducer excitations to prevent oscillation of the input trajectories. In addition, the maximum input amplitude is limited with inequality constraint approximations. The presented feedforward scheme finds the foci points as well as the scanning path in loose sense, since solution of the feedforward control problem does not necessarily lead to foci based solution. In addition, the accumulated thermal dose as the transducers have been switched off is taken into account in control. The presented feedforward control scheme leads to a large dimension nonlinear control problem and it is solved with a gradient based algorithm.

In the second part of the overall control scheme, LQG feedback controller is derived

to compensate the modeling errors which may arise in feedforward part. During the ultrasound surgery, the temperature measurements can be taken from MRI [10]. This temperature data can be used as a feedback for controller. In the proposed feedback scheme the original nonlinear state equation is linearized with respect to the feedforward trajectories for temperature and control input. The standard LQG control and Kalman filter are then derived using the linearized equations.

2 MATHEMATICAL MODELS

The time-harmonic ultrasound field can be characterized with Helmholtz equation in inhomogeneous absorbing media. The Helmholtz equation is

$$\nabla \cdot \left(\frac{1}{\rho} \nabla p \right) + \frac{\kappa^2}{\rho} p = 0, \tag{1}$$

where p is the space dependent part of the pressure field, ρ is the density of the medium and κ is the wave number. In absorbing media the wave number can be expressed as $\kappa = 2\pi f/c + i\alpha$, where f is the frequency and α is the absorption coefficient [2].

In this study the Helmholtz equation is solved with ultra weak variational formalism (UWVF) [4]. The main idea in UWVF is that a priori information of the solution can be included to the approximation subspace. The UWVF formulation for the Helmholtz problem and computational aspects are discussed in [9].

The temperature evolution in tissues can be modeled with the Pennes bioheat equation, which is [20]

$$\rho C_{\mathrm{T}} \frac{\partial T}{\partial t} = \nabla \cdot \kappa \nabla T - w_{\mathrm{B}} C_{\mathrm{B}} (T - T_{\mathrm{A}}) + q, \tag{2}$$

where T is temperature, k is the diffusion coefficient, w_{B} is the perfusion, C_{B} is the heat capacity of blood, T_{A} is the arterial blood temperature and q is the heat source. In this study, the bioheat equation is solved with the semi-discrete finite element method (FEM) and implicit Euler method for temporal integration. The implicit Euler FE form of the bioheat equation can be expressed as

$$T_{t+1} = AT_t + P + M_{\mathrm{D}} (Bu_t)^2, \tag{3}$$

where matrices A and P comes from the standard theory of the FEM and matrix M_D is the modified mass matrix. The matrix B is formed so that the real and imaginary parts of the time-harmonic ultrasound fields from individual transducer elements are separated. The control input vector u has the time-varying coefficients for each real and imaginary part. The details of the FEM formulation for similar control purposes can be found from [16, 17].

In biological tissues the thermal dose $D(T)$ can be calculated as [22]

$$D(T) = \int_0^{t_f} R(T)^{\left(43 - T(t)\right)} h, \qquad R(T) = \begin{cases} 0.25 & \text{for } T(t) < 43^{\circ}\mathrm{C} \\ 0.50 & \text{for } T(t) \geq 43^{\circ}\mathrm{C} \end{cases} \tag{4}$$

The unit of the thermal dose is equivalent minutes in 43°C. The thermal dose that causes necrosis in the most of the soft tissues is reported to be between 50 and 240 equivalent minutes at 43°C [6, 19].

3 FEEDFORWARD CONTROL

The cost function for thermal dose control can be expressed as

$$J(T, \dot{u}) = \frac{1}{2}(D(T) - D_d)^T W (D(T) - D_d) + \frac{1}{2}\int_0^{t_f} \dot{u}_t^T S \dot{u}_t \, \mathrm{d}t, \tag{5}$$

where the difference between the thermal dose and the desired thermal dose D_d is weighted with positive definite matrix W and the time derivative of the control input is weighted with positive definite matrix S.

In practice, the maximum input amplitude of the transducers is limited. This limitation can be handled with inequality constraint approximation, which i$^{\text{th}}$ component can be written as

$$c_i(u_t) = \begin{cases} K\left((u_{i,t}^2 + u_{m+i,t}^2)^{1/2} - u_{\max,\mathrm{k}}\right)^2, & \text{if} \quad \left(u_{i,t}^2 + u_{m+i,t}^2\right)^{1/2} \geq u_{\max,\mathrm{k}} \\ 0, & \text{if} \quad \left(u_{i,t}^2 + u_{m+i,t}^2\right)^{1/2} < u_{\max,\mathrm{k}} \end{cases} \tag{6}$$

where K is weighting scalar and $u_{\max,\mathrm{k}}$ is the maximum amplitude during k^{th} interval of the treatment.

Combining the state equation (3), cost function (5) and inequality constraint approximation for the input amplitude (6) gives the Hamiltonian form, which is

$$\begin{aligned} H(T, u, \dot{u}) \;=\; & \frac{1}{2}(D(T) - D_d)^T W (D(T) - D_d) + \frac{1}{2}\dot{u}_t^T S \dot{u}_t \\ & + \lambda^T \left(AT_t - P - M(Bu_t)^2\right) + \mu^T c(u_t)\,, \end{aligned} \tag{7}$$

where λ is the Lagrange multiplier for the state equation and μ is the Lagrange multiplier for the input amplitude inequality constraint approximation.

The solution to the feedforward control problem can be computed for example with the gradient search algorithm which details can be found from [17, 15]. The algorithm can be divided into following steps: 1) Compute the state equation. 2) Compute the Lagrange multiplier for the state equation. 3) Compute the Lagrange multiplier for the control input inequality constraint 4) Compute the stationary condition (i.e. $\partial H / \partial u_t$). 5) Compute the update for the control input at iteration round ℓ as $u^{\ell+1} = u^\ell + \epsilon(\partial H / \partial u_t)^\ell$, where ϵ is the step parameter. 6) If the change in the cost function (5) is small enough, stop iteration, else return to the step 1).

4 FEEDBACK CONTROL

The modeling errors which may arise in feedforward control affects to the obtained temperature and thermal dose distribution. The modeling errors are mainly in the acoustic parameters of the Helmholtz equation and in the thermal parameters of the bioheat equation. To compensate these errors during the treatment the MRI based temperature feedback can be used on-line during the treatment. In this study, LQG feedback controller and Kalman filter are used for feedback control and state estimation.

The first task in the feedback control is to linearize the nonlinear state equation with respect to the feedforward temperature and control input trajectories. In addition, the feedforward control is computed with time discretization of the order of a second. The MRI imaging sequences are few seconds during ultrasound surgery. To compensate for this difference, the feedback is computed with different time discretization than the feedforward part.

Let the length of the feedforward time discretization be h. In feedback control d steps of feedforward control are taken at once, giving new step length dh. With these changes, the linearized multi-step state equation can be written as

$$\Delta T_{k+1} = \widetilde{F}\Delta T_k + \widetilde{B}_k \Delta u_k \,, \tag{8}$$

where

$$\begin{aligned} \widetilde{F} &= A^d \\ \widetilde{B}_k &= h \sum_{t=kd+1}^{kd+d} A^{t-kd-1} G(u_{0,t}), \end{aligned} \tag{9}$$

and where $G(u_{0,t})$ is the Jacobian of the state equation with respect to the feedforward input trajectory $(u_{0,t})$, ΔT_{k+1} is the linearized temperature and Δu_k is the feedback correction to the input. The cost function for the LQG control can be set as

$$\Delta J = \sum_{k=1}^{N_k} \left((\Delta T_k)^T \, Q \, (\Delta T_k) + \Delta u_k^T \, R \, \Delta u_k \right) . \tag{10}$$

where positive definite matrix Q weights the linearized temperature (i.e. difference between actual temperature and feedforward temperature) and positive definite matrix R weights the input correction.

The LQG feedback controller and the Kalman filter gains are computed from the standard optimal control theory [24] by solving the associated Riccati matrices (for details, see [13, 14]).

In this study, the LQG feedback control and Kalman filter are tested using synthetic data. In feedforward control the acoustic and thermal parameters are adopted from the literature and they are known only approximately. In simulations, different thermal

parameters are used when real system is simulated. In this case the bioheat equation can be written as

$$T_{t+1} = A_r T_t + P_r + M_{D,r}(B_r(u_{0,t} + \Delta u_k))^2, \tag{11}$$

where the feedback correction Δu_k is held constant over the time interval $t \in [k, k+1]$ and subscript r denotes associated FE matrices which are constructed by using the real parameters. In addition, the state estimate is computed with the same discretization (with step length h) as the state equation with original feedforward control matrices, since errors are considered as unknown disturbances to the system. During the time interval $t \in [k, k+1]$, the state estimate is

$$\widehat{T}_{t+1} = A\widehat{T}_t + P + M_D(B(u_{0,t} + \Delta u_k))^2. \tag{12}$$

The corrections for the state estimate and the input are updated after every step k from the measurements and the state estimated feedback using

$$\begin{aligned} y_k &= CT_k + v_k & (13)\\ \widehat{T}_{k+1} &= A\widehat{T}_k + P + M_D(B(u_{0,k} + \Delta u_k))^2 + L(y_k - C\widehat{T}_k) & (14)\\ \Delta u_{k+1} &= -K_{k+1}(\widehat{T}_{k+1} - T_{0,k+1})\,, & (15) \end{aligned}$$

where y_k is the measurement, v_k is the measurement noise, L is the steady state Kalman gain and K_{k+1} is the time-varying LQG feedback gain. The feedback correction is constant during time interval $t \in [k, k+1]$ and piece wise constant during the whole treatment.

5 NUMERICAL STUDIES

5.1 Feedforward control simulations

The reviewed control methods were tested with numerical simulations. The model problem concerns ultrasound surgery of the breast cancer. The computational domain is shown in Fig. 1. The domain is divided into four subdomains which are water (Ω_{I}), skin (Ω_{II}), healthy breast (Ω_{III}) and breast cancer (Ω_{IV}). The acoustic and thermal parameters for subdomains are given in Table 2. The heat capacity of blood was set to 3770 J/kgK in all simulations. The transducer system which was used in simulations was a 20-element phased array. The computational domain was divided into mesh with 2108 vertex nodes and 4067 elements. The frequency of the wave fields was set to 500 kHz. The ultrasound fields were computed with UWVF for each transducer element separately. The solutions were normed so that the maximum amplitude was 1 MPa for all wave fields.

The feedforward control problem was to achieve the thermal dose of 240 equivalent minutes at 43°C in cancer area while keep the thermal dose in healthy tissue below 120 equivalent minutes. Treatment time was set to 180 s and time step h was set to 0.5 s in temporal discretization. Several simulations were accomplished to find suitable weighting for thermal dose distribution. These simulations resulted in following weighting: weighting matrix W was set to a diagonal matrix. The weights were set to 500 for the nodes in the

Domain	α (Nep/m)	c (m/s)	ρ (kg/m^{3}s)	k (W/mK)	C_{T} (J/kgK)	w_{B} (kg/m^{3}s)
Ω_{I}	0	1500	1000	0.60	4190	0
Ω_{II}	12	1610	1200	0.50	3770	1
Ω_{III}	5	1485	1020	0.50	3550	0.7
Ω_{IV}	5	1547	1050	0.65	3770	2.3

Table 1: The acoustic and thermal parameters for the feedforward control simulation.

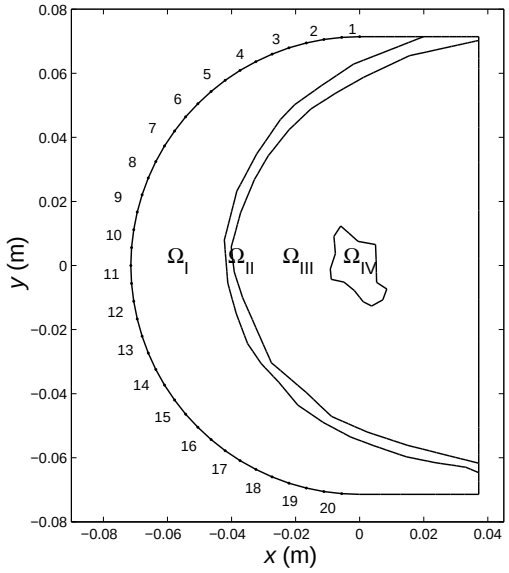

Figure 1: Left: The computing domain with 20 ultrasound transducers located in the left (numbered $1, \ldots, 20$).

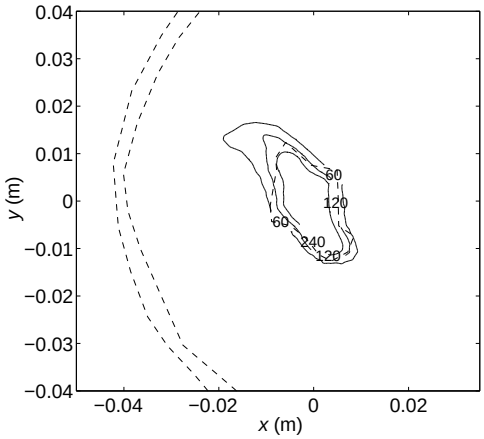

Figure 2: Thermal dose contours for the region of interest from the feedforward control. The anatomical boundaries are presented with the dashed lines.

skin (Ω_{II}), 2500 for the nodes in the breast (Ω_{III}) and 2000 for the nodes in the cancer region (Ω_{IV}). The nodes in the water (Ω_{I}) were weighted with zero.

The input inequality constraint approximation was tested by setting the maximum amplitude $u_{\max,1}$=0.8 MPa for $t = [0, \ldots, 50]$ s and $u_{\max,2}$=0.02 MPa for $t = [50, \ldots, 180]$ s. These criteria mean that when the transducers are on, the amplitude is limited by $u_{\max,1}$, and when the transducers are effectively turned off, the amplitude is limited by $u_{\max,2}$. In inequality constraint the weighting of $K = 50000$ was used to constraint the maximum input amplitude. Another design criteria for input was that the input trajectories was desired to be non-oscillating functions of time. This criterion was satisfies by setting weighting matrix S= diag(10000). The iteration step parameter ϵ was chosen so that the point wise correction to the input was less than 0.01 MPa. The solution to the feedforward control problem was found with algorithm described in Section 3. The algorithm took 1240 iteration rounds with presented parameters to satisfy the stopping criterion, which was that the relative change in cost function was less than 10^{-5}.

The resulting thermal dose contours for the region of the interest is shown in Fig. 2. This figure indicates that the major part of the dose is in the cancerous area, while healthy regions does not get much undesired thermal dose. The thermal dose of 240 equivalent minutes is found in 74.5% of the cancer area, while thermal dose in other regions is reasonable low. The thermal dose of 120 equivalent minutes can be found only from 2.4% of the healthy breast while dose in skin is much lower than 120 equivalent minutes. These results indicate that the design criteria is approximately valid in all subdomains.

Examples of the phase and amplitude trajectories are shown in Fig 3. The amplitude was limited effectively to 0.8 MPa with inequality constraint approximation during the first part of the treatment and to 0.02 MPa during the second part, i.e. when tissue cools. The cooling time is very important in this simulation, since 75% of the thermal

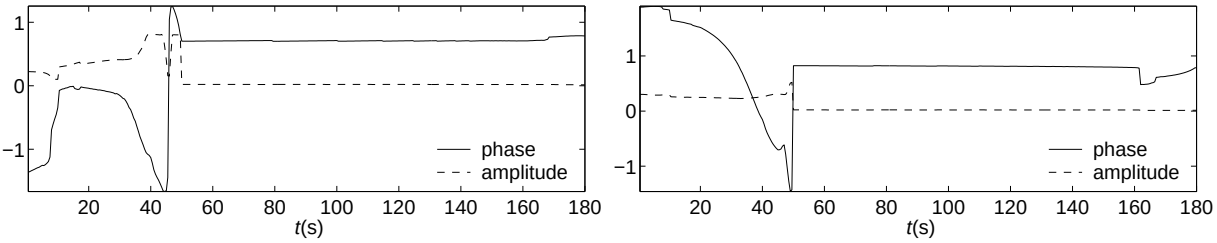

Figure 3: The phases and the amplitudes of the transducer signals from the feedforward control simulation. The figures are for the transducer 3 (left) and 15 (right).

dose was accumulated during the cooling. Finally, there is no violent oscillation in phase and amplitude trajectories so the non-oscillatory penalty is also satisfied.

5.2 Feedback control simulations

The feedback controller and filter were numerically tested using synthetic data. The MRI data acquisition time in ultrasound surgery of the breast are reported to be between 2.3 and 7.2 seconds [11, 3], so the time lag between the temperature measurements was chosen to be 4 s to simulate the MRI imaging sequences. The temperature measurement at each node in the mesh was taken as the mean value of the computed temperature over each 4 seconds interval. The multi-step implicit Euler was adopted by setting d=8 corresponding to a lag of dh=4 s. The LQG feedback controller was derived by choosing the temperature trajectory weighting matrix to $Q = W/1000$ and the weighting for the input correction Δu_k was R =diag(1000). In simulations Gaussian noise with standard deviation of ± 1°C was added to the temperature measurements.

In following, results from the two worst case simulations are presented. These simulations are chosen to simulate the real systems whose acoustic and thermal parameters are not known exactly. In simulation A, the absorption in tissues is dramatically higher than in feedforward control. In simulation B, the absorption is dramatically lower than in feedforward control. Furthermore, other acoustic and thermal parameters are also changed in these simulations.

The acoustic and thermal parameters for feedback simulation A are given in Table 2. The wave fields were solved with UWVF using these parameters. The thermal dose contours with and without feedback are shown in Fig. 4. The higher thermal dose contours without feedback covers large area of the healthy breast, while LQG feedback decreases undesired thermal dose effectively.

The temperature trajectories from simulation A are shown in Fig. 7, which indicates that feedback controller effectively decreases the maximum temperature in both healthy and cancerous tissue.

The acoustic and thermal parameters for feedback simulation B are given in Table 3. In this case absorption was set dramatically lower than what was used in feedforward control. In addition, errors are not homogeneously distributed in tissue, for example

Domain	α (Nep/m)	c (m/s)	ρ (kg/m^{3}s)	k (W/mK)	C_{T} (J/kgK)	w_{B} (kg/m^{3}s)
Ω_{II}	14	1700	1100	0.60	3650	0.8
Ω_{III}	7	1500	980	0.70	3600	0.6
Ω_{IV}	8	1400	1000	0.70	3700	2.0

Table 2: The acoustic and thermal parameters for the feedback control simulation A.

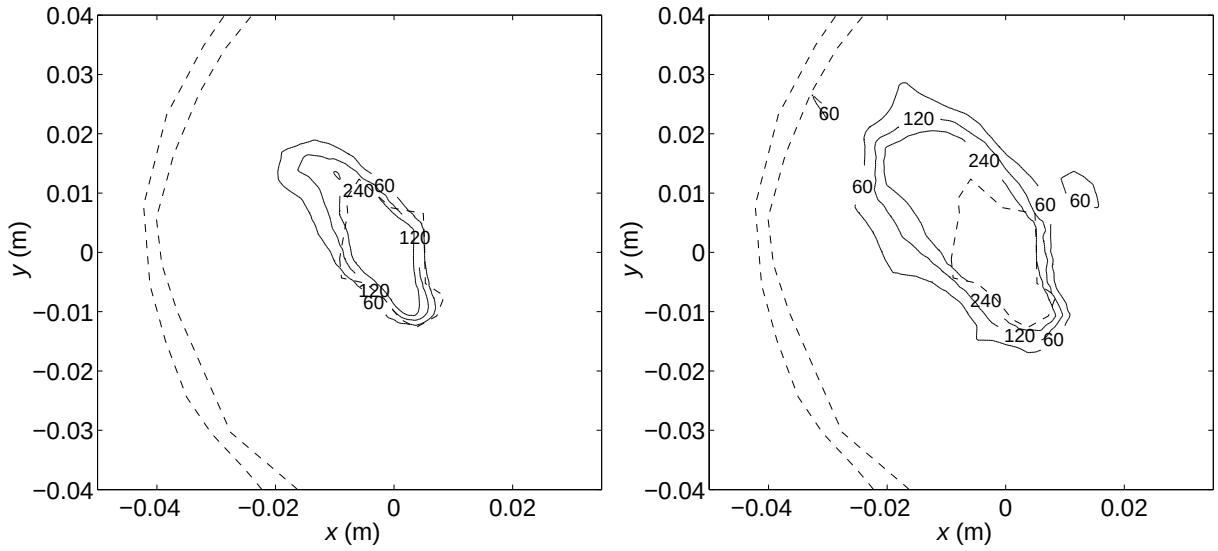

Figure 4: Thermal dose contours from the feedback simulation A. Left: Thermal dose contours with feedback. Right: Thermal dose contours without feedback.

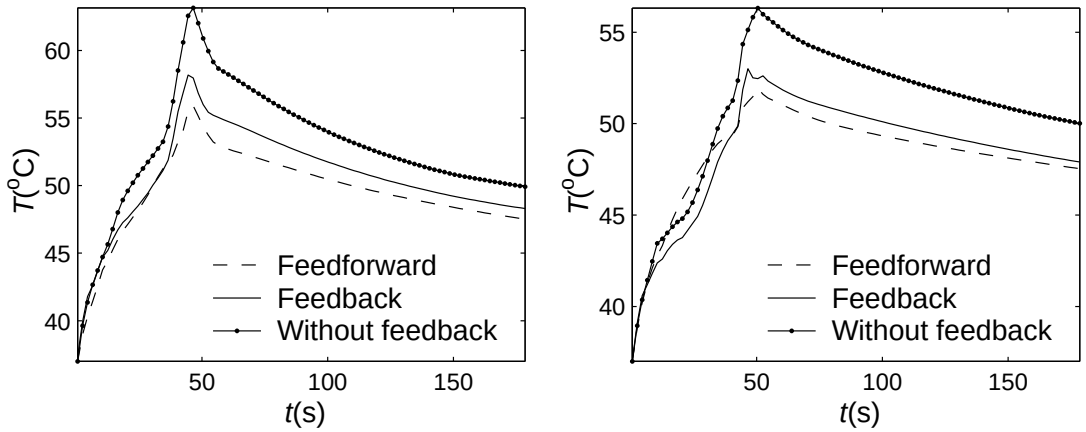

Figure 5: Results from the feedback simulation A. Left: The maximum temperature in the cancer (Ω_{IV}). Right: The maximum temperature in the healthy breast (Ω_{III}).

Domain	α (Nep/m)	c (m/s)	ρ (kg/m^{3}s)	k (W/mK)	C_{T} (J/kgK)	w_{B} (kg/m^{3}s)
Ω_{II}	10	1400	1200	0.70	3570	1.2
Ω_{III}	4	1300	1100	0.60	3750	0.8
Ω_{IV}	3	1680	1100	0.50	3670	1.7

Table 3: The acoustic and thermal parameters for the feedback control simulation B.

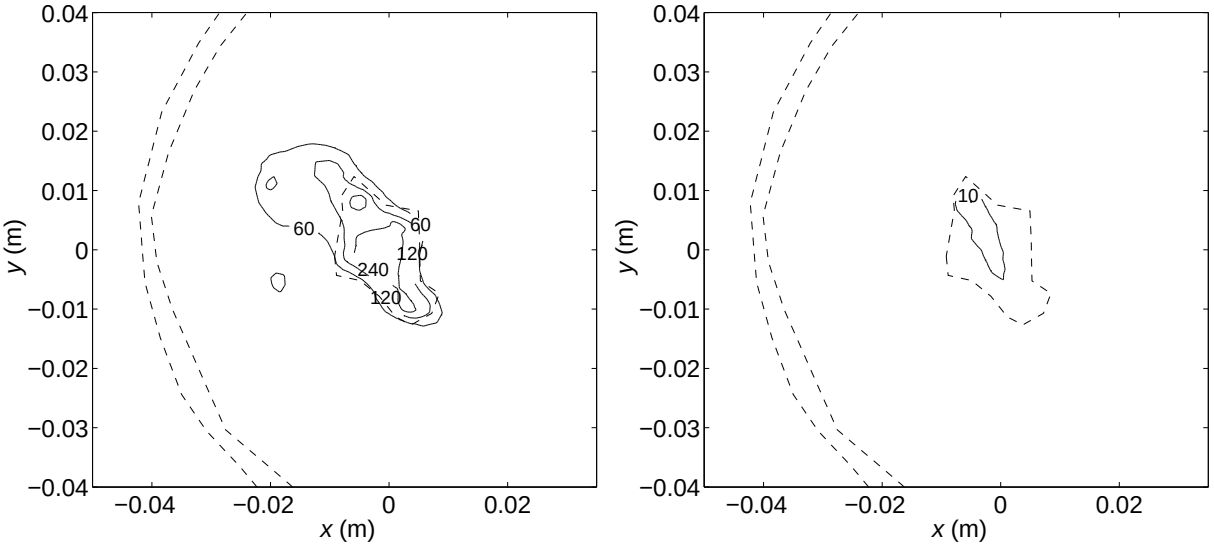

Figure 6: Thermal dose contours from feedback simulation B. Left: Thermal dose contours with LQG feedback. Right: Thermal dose contours without feedback

absorption in breast is set higher than the absorption in cancer. This makes task harder for the feedback controller.

The resulting thermal dose contours with and without feedback are shown in Fig. 6. This figure indicates that the thermal dose contours are dramatically improved with feedback. Even the parameter errors are not homogeneously distributed, a feasible solution could be achieved with feedback.

The temperature trajectories from feedback simulation B are shown in Fig. 7. The feedback controller increases the temperature in all subdomains. However, the maximum temperature in healthy breast causes limitations to temperature increase in cancer.

6 CONCLUSIONS AND DISCUSSION

In this paper a two-stage control method was proposed to control the thermal dose in ultrasound exposures. The presented scheme was numerically tested in 2D simulations.

The results from the simulations show that the feedforward control method is capable for heating large cancer volumes at reasonable treatment time. The thermal dose can be controlled in cancerous tissue as well as in healthy tissue. In addition, the transducer

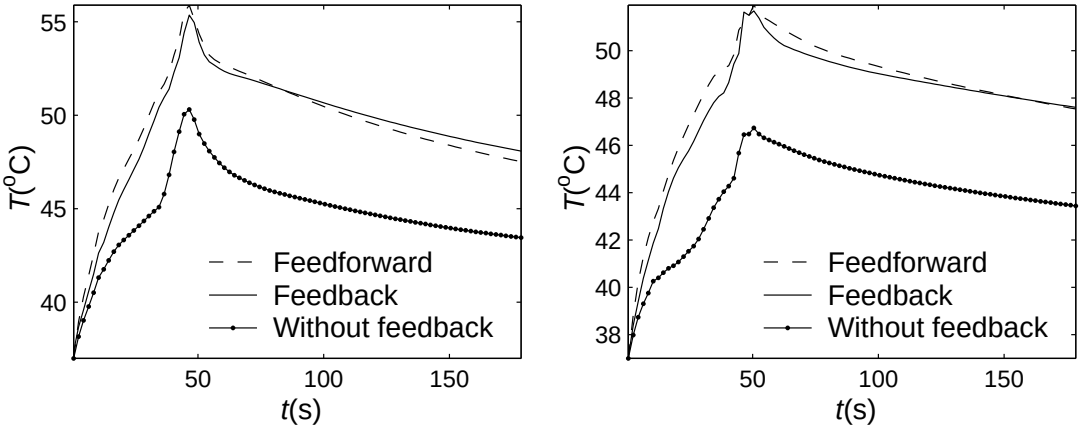

Figure 7: Results from the feedback simulation B. Left: The maximum temperature in the cancer (Ω_{IV}). Right: The maximum temperature in the healthy breast (Ω_{III}).

limitations can be included to control problem. As compared to earlier model-based optimization studies, the proposed feedforward scheme has several advantages. First, the method does not need prefocused ultrasound fields or predetermined scanning path. Furthermore, focusing is usually made under approximation of homogeneous medium, and this can lead to errors if actual field is applied in inhomogeneous media. The proposed control method takes into account the tissue inhomogeneities when solution is computed. Second, diffusion during the treatment is rather advantage than a drawback. Third, Thermal dose accumulation after the transducers have been switched off can be taken into account.

The results from the feedback simulations indicate that the presented scheme is robust. The feedback controller can compensate large modeling errors which are inhomogeneously distributed in tissue. Although the LQG/LQR procedure has been already proposed for temperature control in ultrasound therapy [8, 18, 27], there is a great difference between earlier studies and proposed method. The proposed feedback controller cannot only change the applied power of the ultrasound transducers but also the phase. This is a clear advantage as compared to earlier work, especially when parameter errors in tissues are not homogeneously distributed. In these cases phase correction is necessity to obtain the desired thermal response in tissues.

The future work would be verifying the feedback scheme in 3D. Another topic is verifying the control methods in practice.

7 ACKNOWLEDGEMENTS

This study was supported by the Finnish Academy grants, by the 77818, 72431, 80773, 200627, 44042 and 54065, by the Finnish Cultural Foundation of Northern Savo, by the Foundation of Advanced Technology in Eastern Finland and by Jenny and Antti Wihuri foundation.

REFERENCES

[1] D. Arora, M. Skliar, and R.B. Roemer. Model-predictive control of hyperthermia treatments. *IEEE Transactions on Biomedical Engineering*, 49:629–639, 2002.

[2] A.B. Bhatia. *Ultrasonic Absorption: An Introduction to the Theory of Sound Absorption and Dispersion in Gases, Liquids and Solids*. Dover, 1967.

[3] C. Bohris, J.W. Jenne, R. Rastert, I. Simiantonakis, G. Brix, J. Spoo, M. Hlavac, R. Nemeth, P.E. Huber, and J. Debus. MR monitoring of focused ultrasound surgery in a breast tissue model in vivo. *Magnetic Resonance Imaging*, 19:167–175, 2001.

[4] O. Cessenat and B. Després. Application of an ultra weak variational formulation of elliptic PDEs to the two-dimensional Helmholtz problem. *SIAM Journal of Numerical Analysis*, 35(1):255–299, 1998.

[5] L. Crum and K. Hynynen. Sound therapy. *Physics World*, pages 28–33, August 1995.

[6] C. Damianou and K. Hynynen. The effect of various physical parameters on the size and shape of necrosed tissue volume during ultrasound surgery. *The Journal of the Acoustical Society of America*, 95(3):1641–1649, 1994.

[7] D. R. Daum and K. Hynynen. Thermal dose optimization via temporal switching in ultrasound surgery. *IEEE Transactions on Ultrasonics, Ferroelectrics, and Frequency Control*, 45(1):208–215, 1998.

[8] E. Huthcinson, M. Dahleh, and K. Hynynen. The feasibility of MRI feedback control for intracavitary phased array hyperthermia treatments. *International Journal of Hyperthermia*, 14:39–56, 1998.

[9] T. Huttunen, P. Monk, and J.P. Kaipio. Computational aspects of the ultraweak variational formulation. *Journal of Computational Physics*, 182:27–46, 2002.

[10] K. Hynynen. Focused ultrasound surgery guided by MRI. *Science & Medicine*, pages 62–71, September/October 1996.

[11] K. Hynynen, O. Pomeroy, D.N. Smith, P.E. Huber, N.J. McDannold, J. Kettenbach, J. Baum, S. Singer, and F.A. Jolesz. MR imaging-guided focused ultrasound surgery of fibroadenomas in the breast: A feasibility study. *Radiology*, 219(1):176–185, 2001.

[12] W.L. Lin, T.C. Liang, J.Y. Yen, H.L. Liu, and Y.Y. Chen. Optimization of power deposition and a heating strategy for external ultrasound thermal therapy. *Medical Physics*, 28(10):2172–2181, October 2001.

[13] M. Malinen. *Computational Methods for Optimal Control in Ultrasound Therapy*. PhD thesis, University of Kuopio, 2004.

[14] M. Malinen, S.R. Duncan, T. Huttunen, and J.P. Kaipio. Feedforward and feedback control of ultrasound surgery. *Submitted to Applied Numerical Mathematics*, 2004.

[15] M. Malinen, T. Huttunen, K. Hynynen, and J.P. Kaipio. Simulation study for thermal dose optimization in ultrasound surgery of the breast. *Medical Physics. Accepted for publication*, 2004.

[16] M. Malinen, T. Huttunen, and J.P. Kaipio. An optimal control approach for ultrasound induced heating. *International Journal of Control*, 76:1323–1336, 2003.

[17] M. Malinen, T. Huttunen, and J.P. Kaipio. Thermal dose optimization method for ultrasound surgery. *Physics in Medicine and Biology*, 48:745–762, 2003.

[18] M. Mattingly, R.B. Roemer, and S. Devasia. Exact temperature tracking for hyperthermia: A model-based approach. *IEEE Transactions on Control Systems Technology*, 8(6):979–992, 2000.

[19] N.J. McDannold. *MRI monitoring of high temperature ultrasound therapy.* PhD thesis, Tufts University, 2002.

[20] H.H. Pennes. Analysis of tissue and arterial blood temperatures in the resting human forearm. *Journal of Applied Physiology*, 1:93–122, 1948.

[21] R. Salomir, F.C. Vimeux, J.A. de Zwart, N. Grenier, and C.T.W. Moonen. Hyperthermia by MR-guided focused ultrasound: Accurate temperature control based on fast MRI and a physical model of local energy deposition and heat conduction. *Magnetic Resonance in Medicine*, 43:342–347, 2000.

[22] S.A. Sapareto and W.C. Dewey. Thermal dose determination in cancer therapy. *International Journal of Radiation Oncology, Biology, Physics*, 10(6):787–800, June 1984.

[23] N.B. Smith, N.K. Merrilees, M. Dahleh, and K. Hynynen. Control system for an MRI compatible intracavitary ultrasound array for thermal treatment of prostate disease. *International Journal of Hyperthermia*, 17:271–282, 2001.

[24] R.F. Stengel. *Optimal Control and Estimation.* Dover Publications, Inc., 1994.

[25] G. ter Haar. Acoustic surgery. *Physics Today*, pages 29–34, December 2001.

[26] G.R. ter Haar. Focused ultrasound surgery. In F.A. Duck, A.C. Baker, and H.C. Starrit, editors, *Ultrasound in Medicine*, chapter 9, pages 177–188. Institute of Physics Publishing, 1998.

[27] A. Vanne and K. Hynynen. MRI feedback temperature control for focused ultrasound surgery. *Physics in Medicine and Biology*, 48:31–43, 2003.